

Corrosion Study of Galvanized Steel in Salty Acidic and Basic Solutions

*Khulood Abid Al-Saade and Hayfaa A.Abas **

ABSTRACT

The corrosion of galvanized steel, in hydrochloric acid solution (pH= 2 and 4) and in sodium hydroxide solution (pH= 8 and 10) in the presence of sodium chloride with in concentration range 0.05-1 M, has been studied at temperature range 298-328 K, by using a computerized potentiostat. The weight loss, penetration loss, and cyclic polarization curves data have been evaluated for all states to study the pitting corrosion.

Keywords: Corrosion, Galvanized Steel, Pitting Corrosion.

INTRODUCTION

The corrosion of electro galvanized steel exposed to (0.1) M NaCl was studied using the Scanning Vibrating Electrode Technique SVET. The results show the existence of a defect that accelerated the corrosion process (Bastos, A.C, 2003). The Corrosion resistance of hot dip galvanized steel sheets in a 5% sodium chloride environment was enhanced by an increase in the galvanizing temperature, immersion time and withdrawal speed (Oluwadare, G.O, 2007). Hot dip galvanizing is a metallurgical process whereby perfectly cleaned steel is totally immersed into molten zinc at a temperature of approximately 450°C. During this process the carbon steel metallurgically reacts with the molten zinc forming a series of zinc/iron alloys that are chemically bonded to the parent steel leaving atop pure zinc layer (Wilmot, R.E, 2007). These series of zinc/iron alloy layers comprise the thin **Gamma** layer composed of an alloy that is 75% zinc and 25% iron, the **Delta** layer composed of an alloy that is 90% zinc and 10% iron, the **Zeta** layer composed of an alloy that is 94% zinc and 6% iron and the outer **Eta** layer that is composed of pure zinc as shown in (American Galvanizers Association, 2000).

The corrosion behavior of industrial and laboratory zinc coatings was studied in NaCl media under various conditions. The results show that both interfacial

reactions and dissolution processes occur in these media (Hamlaoui, Y, 2007). A pitting corrosion mechanism involving a series of processes from anion competitive adsorption to penetration to nucleation and growth was proposed (Miao, W, 2007). Monitoring of initial stages of atmospheric zinc corrosion simulated acid rain solution under wet-dry cyclic conditions. The experimental results show a pronounced dependence of the reciprocal of polarization resistance on the relative humidity (El Mahdy, G.A, 2004). Pitting corrosion is influenced by many different physicochemical parameters, including the environment, metal composition, potential, temperature and surface conditions. Important environmental parameters include aggressive ion concentration, pH and inhibitor concentration (Frankel, G.S, 1987). The mechanism of pitting corrosion was illustrated schematically in Fig. 1 which indicates a metal M being pitted by an aerated sodium chloride solution. Rapid dissolution occurs within the pit, while oxygen reduction takes place on adjacent surfaces. This process is self-stimulating and self-propagating. The rapid dissolution of metal within the pit tends to produce an excess of positive charge in this area, leading to the migration of chloride ions to maintain electrical neutrality. Thus, in the pit there is a high concentration of MCl and, as a result of hydrolysis, a high concentration of hydrogen ions. Both hydrogen and chloride ions stimulate the dissolution of most metals and alloys, and the entire process accelerates with time. In contrast, cathodic oxygen reduction on the surface adjacent to pits tends to suppress corrosion (Fontana, M.G. 1986).

* Department of Chemistry, College of Science, Bagdad University, Iraq. Received on 19/9/2012 and Accepted for Publication on 21/3/2013.

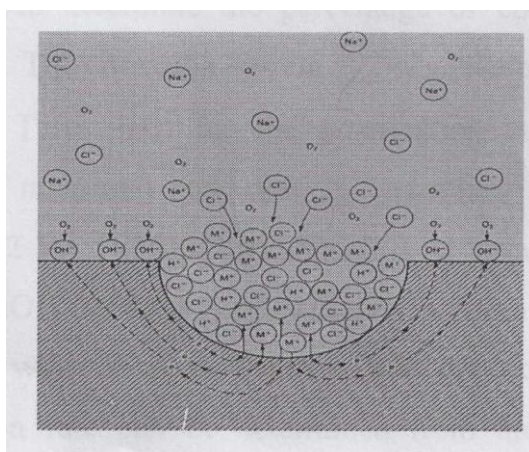


Fig. 1: Autocatalytic process occurring in a corrosion pit

Experimental Procedure

Materials and chemical

The galvanized steel which has been used in this work

had the following composition. The base metal is carbon steel with a typical composition that is given by

<i>P</i>	<i>S</i>	<i>Mn</i>	<i>Si</i>	<i>Co</i>	<i>Metal</i>
0.015	0.015	0.80	0.25	0.40	wt%

The coated layer was a zinc applied with hot- dip method having a thickness = 0.080 nm, the composition of zinc layer was:

Metal	Zn	Al	Sn
Wt %	99	0.5	0.5

Another material has been used for preparation the cell solution:

Material	Supplied from	%purity
Sodium hydroxide	BDH	96.0
Sodium chloride	BDH	99.99
Hydrochloric acid	FLUKA	37

Galvanized steel pieces of 1 cm² area served as the working electrode, platinum served as the counter electrode, while standard calomel electrode (SCE) was used as the reference electrode. The electrochemical studies were conducted using an advanced potentiostat, Winking MLab-200 user (2007) (Germany). [Bank Elektronik-Intelligent]. In this study, the effects of adding different sodium chloride concentration to HCl acid solutions 2 and 4 and sodium hydroxide solutions 10 and 12 on the corrosion of galvanized steel (G-S) has been investigated in order to determine the percentage of corrosion accelerating at different temperatures. The corrosion current *i*_{corr} was evaluated by extrapolating the

anodic and cathodic Tafel lines for the polarization curves. The open circuit potential (OCP) was measured and the polarization curves were scanned between 1.00 and -0.2 V. The HCl solution (0.1 M) was prepared by using HCl (36% Aldrich) and NaOH (99.99% Aldrich) stock solution (0.1M). Each solution prepared by dilution with DI water (with a measured conductivity less than 2 μS/cm). The corrosion rate can be determined from the polarization resistance using the Stern-Geary equation, provided that the polarization resistance (PR) is similar to the charge transfer resistance and the Tafel slopes are known (Frankel, G.S, 2008). The most common way to determine PR is by the linear polarization resistance

(LPR) method, in which the potential is scanned about $\pm 5-10$ mV relative to the corrosion potential, and by

applying the Tafel extrapolation method as shown in Fig. 2 (Murgulescu, I.G, 1961).

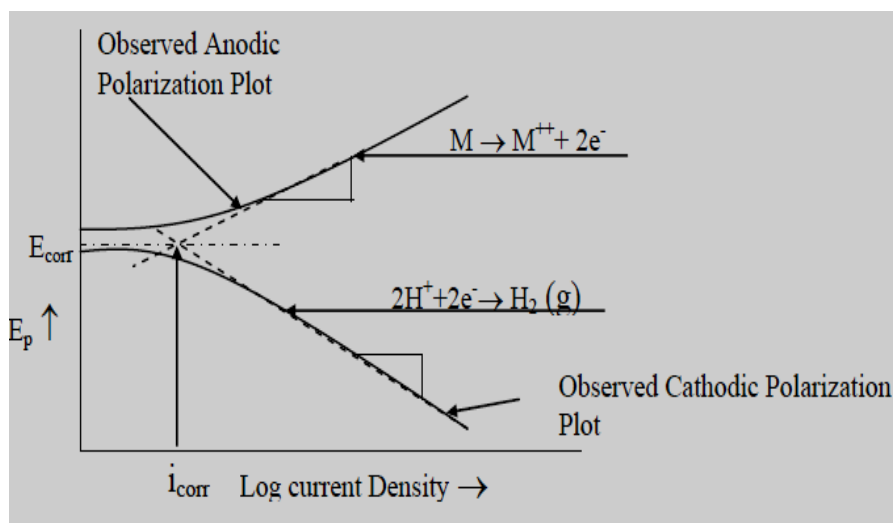


Fig. 2: Semi logarithmic polarization curves for a corrosion system under activation control (Tafel behavior)

Result and Discussion

Fig (3a) shows the relationship between the G.S. corrosion current densities i_{corr} and pH in the temperature range 298-328 K. The i_{corr} values decreased sharply to a minimum then increasing thereafter with increasing pH to attain a maximum. This variation of i_{corr} values reflects the kinetic behavior of the corrosion process. The rate of corrosion being higher in the acidic medium decreasing with decreasing acidity attaining minimum values, increasing thereafter as the medium became basic.

Fig (3-b,c,d,f) shows the variation of the corrosion current densities i_{corr} with pH at constant temperature, but different NaCl concentrations (0.05,0,1,0,5 and 1M) for G.S. The rate of corrosion being higher in the acidic medium ($pH < 4$) and high NaCl concentration decreasing with decreasing acidity and decreasing NaCl concentration to minimum values at pH 4, then slightly rising thereafter with increasing pH up to pH 10, then generally falling beyond that (except for high NaCl concentration at 298K). The variation of i_{corr} values with medium pH and NaCl concentration reflects corrosion

processes which are accelerated by destruction the protective layer at the G.S. surface in a strong acidic and basic medium, while the corrosion in moderate acidic and basic media remain cathodically hindered by zinc (top layer) (Hinds, 1908).

Fig 4 a shows the corrosion potential E_{corr} of G.S. plotted versus pH at four temperatures. E_{corr} values generally moved to less negative values with increasing pH, decreasing thereafter as the medium became basic and as the basal increased. Fig (4-b, c, d.f) show the variation of the corrosion potential for G.S. with pH at constant temperature within the range 298 and 328 K and different NaCl concentration (0.05-1M). It shows that the E_{corr} values decreased to minimum, increasing thereafter with increasing pH. The shift of the corrosion potential in the noble direction (or to a less negative potential) implies generally the tendency of the G.S. specimen for corrosion under certain condition with expected to decrease on purely thermodynamic ground. The variation of E_{corr} reflect the heterogeneous reaction on G.S. surface (Bockris, J.O.M. and Reddy, A.K.N. 1970).

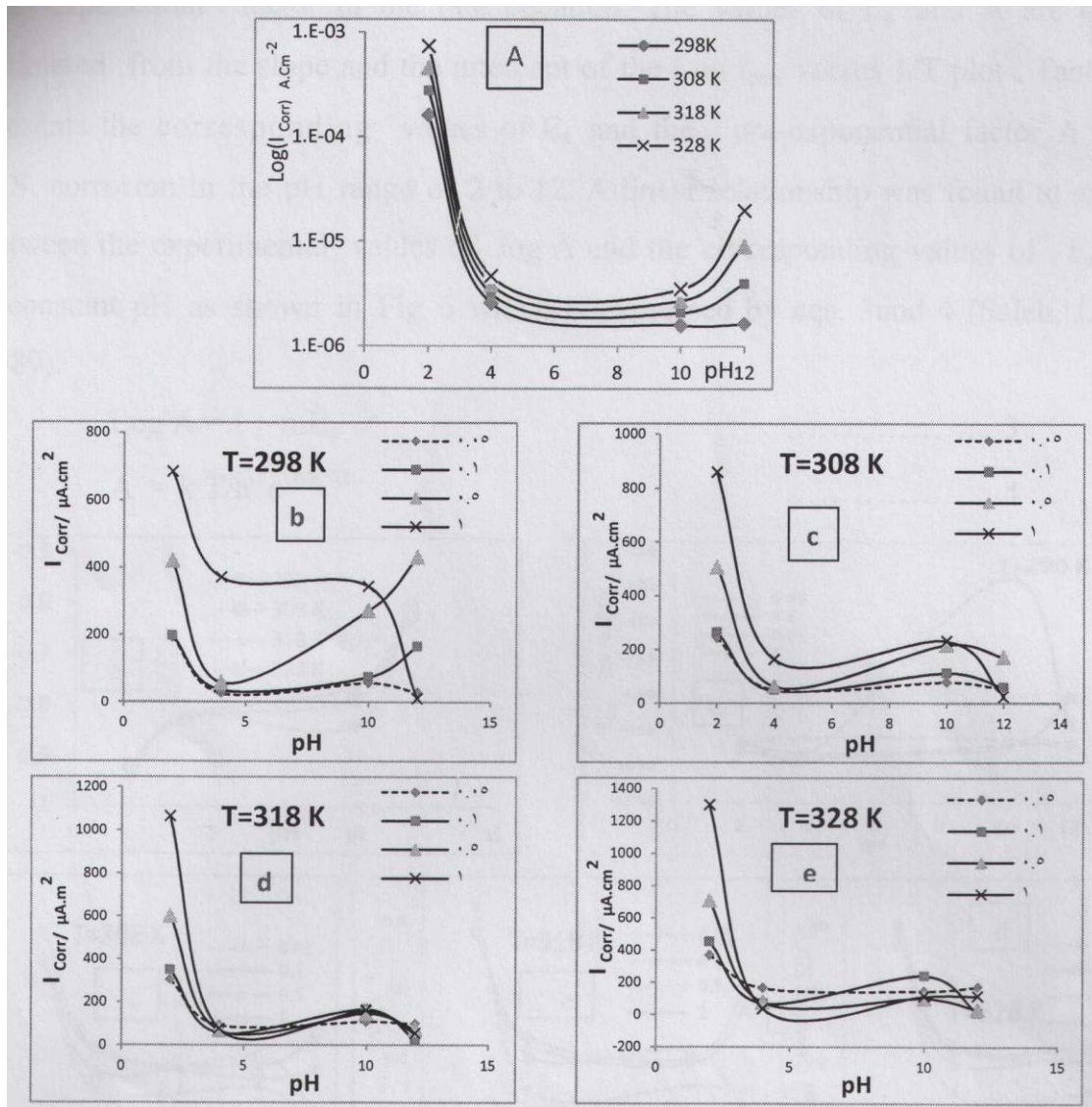


Fig. 3: Variation of the corrosion current densities against pH in different NaCl concentration

The effect of temperature on the rate of corrosion has been studied over the temperature range from -298-328-K. Fig 5 shows plots of Log i_{corr} against the reciprocal of the absolute temperature ($1/T$) for G.S. corrosion in the pH range 2 to 12. The results indicate linear dependence of the Log i_{corr} on $1/T$, which is given by eq. 1 below (Al-Shamma, L.M, 1987).

$$\text{Log } i_{corr} = \text{log } A - E_a / 2.303RT \quad \dots\dots\dots 1$$

which is similar to the linear form of the well-known Arrhenius equation given by eq. 2 below

$$r = A \exp (-E_a/RT) \quad \dots\dots\dots 2$$

Where E_a represents the activation energy of the

corrosion and A is the pre- exponential factor in the rate equation. The values of E_a and A are thus estimated from the slope and the intercept of the Log i_{corr} versus $1/T$ plot. Table 1 presents the corresponding values of E_a and the pre-exponential factor A for G.S. corrosion in the pH range of 2 to 12. A linear relationship was found to exist between the experimental values of log A and the corresponding values of E_a at a constant pH as shown in Fig 6 which is expressed by eqs. 3 and 4 (Saleh, J.M, 1989).

$$\text{Log } A = I + mE_a \quad \dots\dots\dots 3$$

$$A = k T/h e^{\Delta S^*/R} \quad \dots\dots\dots 4$$

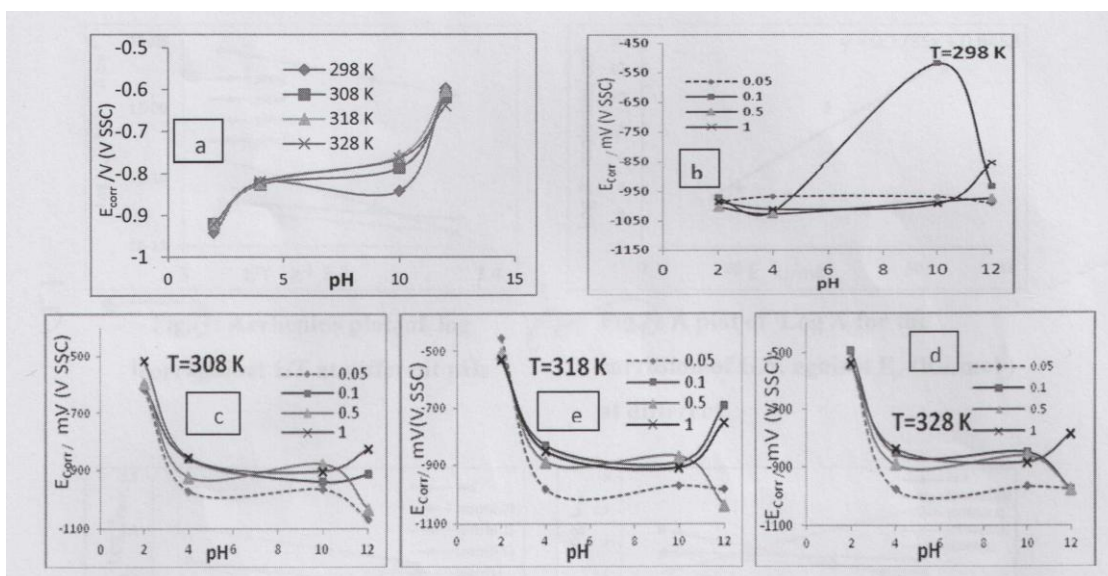


Fig 4: Variation of corrosion potential against pH at different NaCl concentration at constant temperature, for each of the four different temperature 298,303,318 and 328K

Where m and I are respectively the slope and intercept of the plots in Fig 6. Such a relationship reflects a "compensation effect" which is frequently found to describe the kinetics of catalytic and tarnishing reactions on metal (Bockris, J.O.M, 1970). Equation 3 shows that simultaneous increases or decreases in E_a and $\log A$ for a particular system tend to compensate from the standpoint of the reaction rate. When such a compensation operates, it is possible for striking variation in E_a and $\log A$ through a series of surface sites on the metal that exhibit only a small variation in reactivity. Fig. 8 shows the plots of $\log A$ against E_a for G.S. corrosion at constant pH for each of the pHs 2,4,10 and 12 and NaCl concentrations.

The entropy of activation (ΔS^*) was calculated from the value of A using eq. 4.

Where the activated complex represents a more probable arrangement of molecules than found in the normal reactant, ΔS^* is positive and the reaction rate will be higher than normal. Conversely, if the activated complex occurs only after considerable rearrangement of the structure of the reactant molecules, making

the complex a less probable structure, ΔS^* is negative, and the reaction rate will be comparatively lower (Sinko, P.J, 2000).

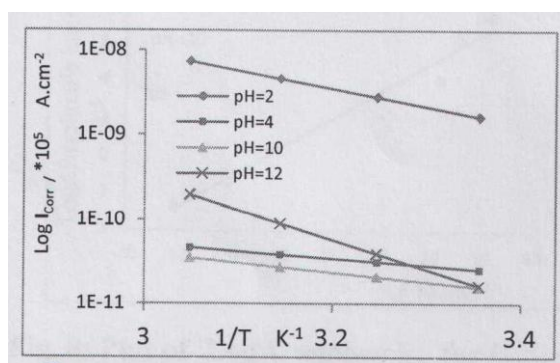


Fig.5: Arrhenius plot, of $\log i_{corr}$ against $1/T$ at different pHs

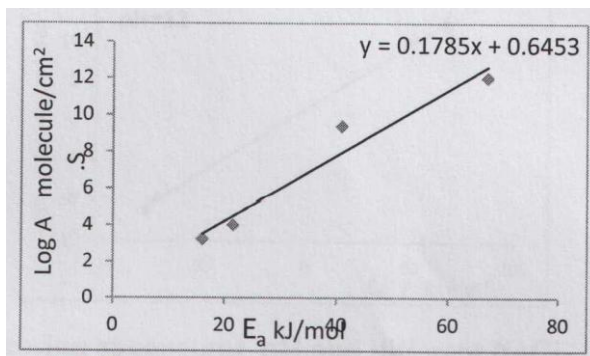


Fig.6: A plot of Log A for the corrosion of G.S. against E_a (KJ/mol) at different NaCl concentrations

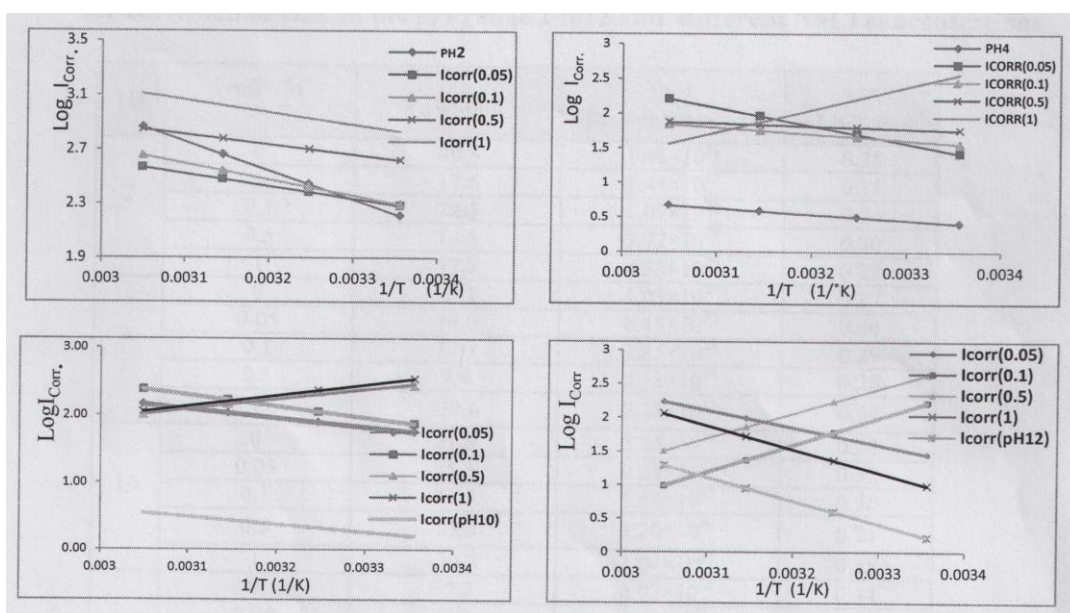


Fig. 7: Arrhenius plots of Log i_{corr} against $1/T$ for the corrosion of G.S. in the pH range 2 to 12 at different NaCl concentrations

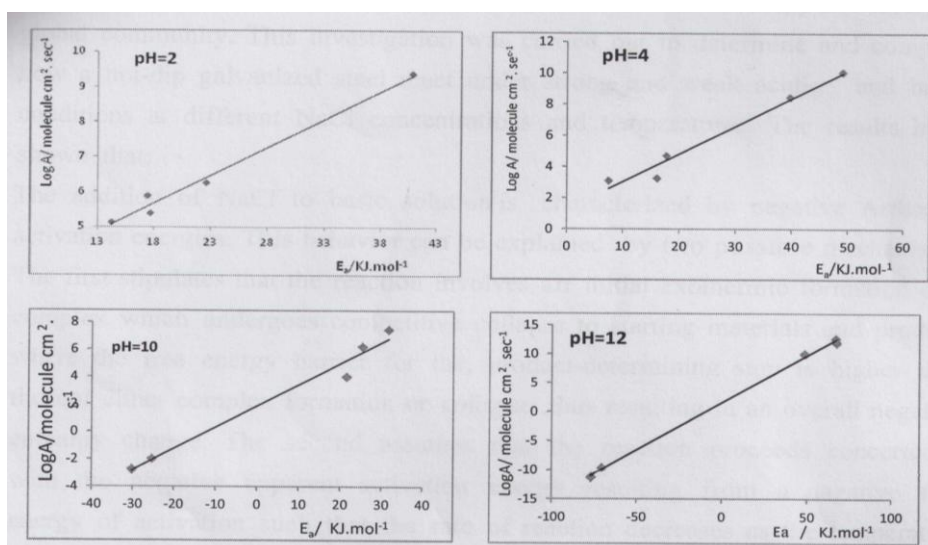


Fig. 8: Plot of Log A against E_a for G.S. corrosion at constant pH and different NaCl concentrations for the PHs at 2,4,10 and 12.

Table 1. Activation energy (E_a), pre-exponential factor (A) and entropy of activation (ΔS^*) for the corrosion of G.S. in the pH range 2 to 12 and different NaCl concentrations

pH	NaCl /M	E_a /kJ.mol ⁻¹	A / Molecule.cm ⁻² . s ⁻¹	ΔS^* /kJ.K ⁻¹ .mol ⁻¹
2	0	40.8	1.43×10^{33}	0.38
	0.05	17.6	1.44×10^{29}	0.31
	0.1	22.5	1.07×10^{30}	0.24
	0.5	14.1	7.77×10^{28}	0.30
	1	17.3	4.58×10^{29}	0.32
4	0	16.1	1.03×10^{27}	0.27
	0.05	49.0	6.45×10^{33}	0.40
	0.1	17.7	2.85×10^{28}	0.29
	0.5	7.4	7.12×10^{26}	0.26
	1	-39.6	2.23×10^{15}	0.04
10	0	21.6	5.86×10^{27}	0.28
	0.05	25.3	9.54×10^{29}	0.32
	0.1	31.7	1.64×10^{31}	0.35
	0.5	-25.3	1.20×10^{24}	0.21
	1	-30.2	1.04×10^{21}	0.15
12	0	67.2	6.02×10^{35}	0.44
	0.05	48.5	5.5×10^{33}	0.40
	0.1	-76.7	3.46×10^{12}	-0.004
	0.5	-70.2	1.28×10^{14}	0.02
	1	66.7	2.95×10^{36}	0.45

Conclusion

The service life of G.S. is of great importance to the economy and safety of global community. This investigation was carried out to determine and compare how a hot-dip galvanized steel react under strong and weak acidic and basic conditions at different NaCl concentrations and temperatures. The results have shown that:

1. The addition of NaCl to basic solution is characterized by negative Arrhenius activation energies. This behavior can be explained by two possible mechanisms. The first stipulates that the reaction involves an initial exothermic formation of a complex which undergoes competitive collapse to starting materials and product, where the free energy barrier for the, product-determining step is higher than those of either complex formation or collapse, thus resulting in an overall negative enthalpy change. The second assumes that the reaction proceeds concertedly, with the negative apparent activation energy resulting from a negative free energy of

activation such that the rate of reaction decreases as the temperature increases. However the rates of G.S. corrosion generally increase with increasing temperature and pH.

2. G.S. corrosion starts in localized regions, moving to adjacent areas as the zinc consumed in earlier sites, with the speed of corrosion dependent on the type, quality and mode of precipitation of corrosion products. In the absence of NaCl, the zinc corrosion products of the Eta layer in strong acid are readily soluble in water. In strong alkaline solutions, water-soluble products are formed. This does accelerate the corrosion process, not only by destroying the corroded protective layer at the G.S. surface, but also by exposing steel that has to be protected. This speeds up the G.S. corrosion rate.

3. During galvanizing process a series of zinc/iron alloys form with a top pure zinc layer, These layer with its composition accelerate the corrosion process.

4. At high NaCl concentration presence, the rate of G.S. corrosion decreases with increasing temperature, specifically in basic solution because after zinc

consumption, the steel that became exposed remained cathodically protected by zinc.

5. The addition of NaCl to basic solution is

characterized by negative Arrhenius activation energies. This behavior is explained (I).

REFERENCES

- American Galvanizers Association. 2000. Galvanizing for Corrosion Protection- *A Specifier Guide*, P.5-7.
- Al-Shamma, L.M.; Saleh, J.M. and Hikmat, N.A. 1987. Adsorption of carbon disulphide and hydrogen sulphide on evaporated metal films. *J. Corros. Sci*, 27: 221.
- Bastos, A.C.; Simões, A.M. and Ferreira, M.G. 2003. Corrosion of electrogalvanized steel in 0.1 M NaCl studied by SVET. *Portugaliae Electrochimica Acta*, 21: 371-387.
- Bockris, J.O.M. and Reddy, A.K.N. 1970. *Modern Electrochemistry*, Plenum Press, New York, 2: 883.
- El Mahdy, G.A. and Kim, K.B. 2004. Monitoring of initial stages of atmospheric zinc corrosion in simulated acid rain solution under wet-dry cyclic condition, *J. of Corrosion Science and Technology*, 3(6): 251-256.
- Fontana, M.G. 1986. *Corrosion engineering*, McGraw-Hill book Company, Third Edition, 66-67.
- Frankel, G.S. 2008. Electrochemical techniques in corrosion: Status, limitations and needs, *Journal of ASTM International*, 5(2): 101241.
- Frankel, G.S. Stockert, L. Hunkeler, F. and Boehni H. 1987. *Corrosion, Pitting Corrosion*, 43: 429.
- Hamlaoui, Y.; Pedraza, 2F and Tifouti, 3L. 2007. Comparative Study by Electrochemical Impedance Spectroscopy (EIS) On the Corrosion Resistance of Industrial and Laboratory Zinc Coatings, *American Journal of Applied Sciences*, 4(7): 430-438.
- Hinds and Dillard, J. I. 1908. *Inorganic Chemistry, With the Elements of Physical and Theoretical Chemistry* (2nd Ed.), New York: John Wiley and Sons, 506-508.
- Murgulescu, I.G. and Radovici, O. 1961. *Metal corrosion*, 2nd Int. Congr, Butterworths, London, P. 202-205.
- Miao, W.; Coleb, I.S.; Neufeld, A.K. and Furman, S. 2007. Pitting Corrosion of Zn and Zn-Al Coated Steels in pH (2 to 12) NaCl Solutions, *Journal of the Electrochemical Society*, 154(1): 7-15.
- Oluwadare, G.O. 2007. Evaluation of influence of process variables on the corrosion performance of Hot-dip-galvanized steel sheets, *Academic Journals Trends in Applied Sciences Research*, 2(4): 320-326.
- Wilmot, R.E. 2007. Corrosion protection of reinforcement for concrete structures. *The Journal of the Southern African Institute of Mining and Metallurgy*, 107: 139-146.
- Saleh, J.M. and Al-Haidari Y.K. 1989. *Bull. Chem. Soc.*, JPn, 62: 1237.
- Sinko, P. J. 2000. *Physical Chemical and Biopharmaceutical Principles in the Pharmaceutical Sciences*, Fifth Ed, USA, P. 413.

دراسة تآكل الفولاذ المغلون (الفولاذ المطلي بالزنك) في الأوساط الملحية الحامضية والقاعدية

خلود عبد صالح السعدي وهيفاء عبد الامير عباس*

ملخص

جرت دراسة تآكل الفولاذ المغلون (الفولاذ المطلي بالزنك) في محلولي حامض الهيدروكلوريك ذوي الاس الهيدروجيني (2 و4) وفي محلولي هيدروكسيد الصوديوم ذوي الاس الهيدروجيني (8 و10) بغياب وبوجود ملح كلوريد الصوديوم بمدى التركيز (0.05-1) مولاري، كما تمت الدراسة ضمن المدى الحراري 298 الى 328 كلفن وباستخدام المجهاد الساكن الكومبيوتري، حيث تمت متابعة فقدان الوزن والفقدان الناجم عن الاختراق وجرى الحصول على منحنيات الاستقطاب الحلقي وذلك بهدف تقييم مدى التآكل النقري للمحاليل المذكورة اعلاه.

الكلمات الدالة: تآكل، الفولاذ المغلون (الفولاذ المطلي بالزنك)، التآكل النقري.

* كلية العلوم، جامعة بغداد، العراق. تاريخ استلام البحث 2012/6/25 وتاريخ قبوله 2012/10/8.